Biosensors and Bioelectronics 54 (2014) 634–639

Contents lists available at ScienceDirect

Biosensors and Bioelectronics

journal homepage: www.elsevier.com/locate/bios

Simultaneous electrochemical detection of cervical cancer markers using reduced graphene oxide-tetraethylene pentamine as electrode materials and distinguishable redox probes as labels

Dan Wu, Aiping Guo, Zhankui Guo, Lili Xie, Qin Wei*, Bin Du

Key Laboratory of Chemical Sensing & Analysis in Universities of Shandong, School of Chemistry and Chemical Engineering, University of Jinan, Jinan 250022, China

ARTICLE INFO

Article history:
Received 27 August 2013
Received in revised form
30 October 2013
Accepted 12 November 2013
Available online 23 November 2013

Keywords:
Au@mesoporous carbon CMK-3
Simultaneous electrochemical detection
Redox probe
Tumor markers
Reduced graphene oxide-tetraethylene pentamine (rGO-TEPA)

ABSTRACT

A novel, highly sensitive electrochemical immunoassay was proposed for the simultaneous determination of carcinoembryonic antigen (CEA) and squamous cell carcinoma antigen (SCCA) for the diagnosis of cervical cancer. Using an electrochemical analysis technique, two well-separated peaks were generated by neutral red and thionine, making the simultaneous detection of the two analytes on the electrode possible. Reduced graphene oxide-tetraethylene pentamine (rGO-TEPA), containing more amino groups, was of benefit to immobilize the primary antibody (Ab_1) through an amidation reaction. Au@mesoporous carbon CMK-3 was synthesized and incubated with two secondary antibodies (Ab_2) and different redox probes (neutral red and thionine) to fabricate the electrochemical immunosensor label intending to improve the analytical performance of the immunosensor. The immunosensor was prepared with a sandwich structure based on the peak current change of neutral red and thionine before and after the antigen–antibody reaction. The results showed that the immunosensor had a wide linear range, low detection limit, good reproducibility and stability. The method has been applied to the analysis of serum samples with satisfactory results.

1. Introduction

Cancer of the uterine cervix is the major cause of death from gynecologic cancer worldwide. Reported incidence rates in developing countries are much higher than those in developed countries. Precise and early diagnosis of tumor markers could improve the treatment rate of cervical cancer. However, the measurement of a single tumor marker often has limited diagnostic value because no single tumor marker is sensitive and specific enough to meet the strict diagnostic criteria in clinical diagnosis (Li et al., 2011). Moreover, most cancers have more than one tumor marker associated with them (Wilson and Nie, 2006). Therefore, simultaneous detection of multiple analytes has more importance in clinical applications since it can shorten analytical time, decrease detection cost and improve the test efficiency.

Until now, simultaneous electrochemical detection of multiple analytes has been carried out using aptamer-based sensors, screen-printed electrodes, multicolor quantum dots and different electrochemical redox probes (Tian et al., 2012; Guo et al., 2013; Song et al., 2010; Wang et al., 2013; Ma et al., 2013). For example, Zhang's group developed a dual-functional aptamer DNA sequence for the detection of adenosine and thrombin by coupling the enhancement of bio-barcode technology and anodic stripping voltammetry (Li et al., 2010). Ying's group used a high-performance screen-printed graphene electrode to simultaneously determine ascorbic acid, dopamine and uric acid (Ping et al., 2012).

Tumor markers that may be helpful in the management of patients with cervical cancer are squamous cell carcinoma antigen (SCCA) and carcinoembryonic antigen (CEA) (Geyer and Kleine, 1987). SCCA is a subfraction of the tumor antigen TA-4 and was isolated from a squamous cell carcinoma of the uterine cervix. Serum concentrations of SCCA have been found to correlate with tumor stage, tumor size, residual tumor after treatment, recurrent or progressive disease, and survival in patients with squamous cell cervical cancer. Serum determination of SCCA is a useful tool in staging, monitoring of therapy and diagnosing recurrence in squamous cell carcinoma of the cervix (Massuger et al., 1997). CEA (an oncofetal antigen) determinations are valuable in the planning of treatment and follow-up of patients with adenocarcinoma of the cervix (Kjorstad and Ørjasaeter, 1984).

Reduced graphene oxide (rGO) is often used in electrochemical sensors (Zhang et al., 2013; Gan et al., 2011; Huang et al., 2013; Kaur et al., 2013; Liu et al., 2012a; Sun et al., 2013; Teymourian et al., 2013) because (1) its abundant defects and chemical groups

* Corresponding author. Tel.: +86 531 82765730; fax: +86 531 8276 5969.
E-mail address: sdjndxwq@163.com (Q. Wei).

0956-5663/$ - see front matter © 2013 Elsevier B.V. All rights reserved.
http://dx.doi.org/10.1016/j.bios.2013.11.042

facilitate charge transfer and thus ensure high electrochemical activity; (2) the populated chemical moieties on the rGO surface offer the convenience and flexibility for various functionalizations to enhance the sensor performance; (3) the chemical and electrical properties of rGO are highly tunable; and (4) as compared to non-conductive GO, rGO can efficiently transport charges (Liu et al., 2012b). Meanwhile, rGO may also be functionalized through covalent or non-covalent methods in order to further enhance its sensitivity, specificity, loading capacity, biocompatibility, etc. Reduced graphene oxide-tetraethylene pentamine (rGO-TEPA) is a novel material which is a combination of rGO and tetraethylene pentamine through covalent bonding. It not only keeps the original property of rGO but also promotes water solubility. In addition, rGO-TEPA has a large number of amino groups which can form covalent bonds with antibodies to easily enhance the performance of rGO-TEPA. Thus, in order to enhance the sensitivity of the sensor, functionalized rGO nanomaterial-rGO-TEPA was introduced in the fabrication of a sandwich-type electrochemical immunosensor. The structure of rGO-TEPA is shown in Fig. S1.

Due to its unique features, such as good electrical conductivity, good biocompatibility, large specific surface area and tunable porosity, ordered mesoporous carbon (OMC) is a novel material for applications in catalysis, sensing and energy storage (Dai et al., 2012; Zhou et al., 2007a, 2007b; Hartmann 2005). Among OMC materials, CMK-3 has attracted much attention and is obtained by replicating well ordered mesoporous silica, SBA-15. The mesoporous carbon possess a highly ordered 2D hexagonal structure with excellent textural characteristics (Kuppan and Selvam, 2012). In this paper, Au@mesoporous carbon CMK-3 was synthesized and used to adsorb secondary antibodies (Ab_2) (Huang et al., 2010b). The introduction of Au nanoparticles can not only enhance the amount of antibodies immobilized, but also preserve the activity of the immobilized biomolecules, further optimizing the immunosensing performance.

It is well known that, due to the lack of electrochemical activity of the antibodies or antigens, most of the electrochemical immunosensors involve the use of some mediators or labeling of either the antigen or antibody to achieve electron-transfer (Wu et al., 2009). The phenazine dye, neutral red and other phenazine derivatives, particularly toluidine blue, prussian blue, methylene blue, azure A, thionine have been considered as redox mediators for electrochemical investigations of biological systems, due to their low cost and efficient electron transfer (Savari et al., 2013). Using the two cervical cancer biomarkers, SCCA and CEA as model analytes, we developed a novel sandwich immunosensor for the simultaneous determination of multiple analytes by combining the signal amplification strategy with the multiple-label method in this work. As electrochemical redox probes, neutral red and thionine with well-separated peaks were used to label two different antibodies, which were loaded together onto Au@mesoporous carbon CMK-3. Enhanced sensitivity was achieved by using the large specific surface area of rGO-TEPA to increase Ab_1 loading, the large surface area of Au@mesoporous carbon CMK-3 to increase Ab_2 and redox probe loading, and the high conductivity of rGO-TEPA to promote electron transfer. No obvious cross-reactivity was observed during a series of analyses to detect target analytes.

2. Experimental

2.1. Materials and reagents

Reduced graphene oxide-tetraethylene pentamine (rGO-TEPA) and mesoporous carbon CMK-3 were purchased from Nanjing XFNANO Materials TECH Co., Ltd. (China). CEA, SCCA and corresponding antibodies were purchased from Shanghai Linc-Bio Science Co. Ltd. (China). Bovine serum albumin (BSA, 96–99%) was purchased from Sigma (USA) and used as received. Neutral red, thionine, 1-ethyl-3-(3dimethylamino-propyl) carbodiimide (EDC) and *N*-hydroxysuccinimide (NHS) were obtained from the Sinopharm Chemical Reagent Co., Ltd (China). $HAuCl_4 \cdot 3H_2O$ was obtained from Sigma-Aldrich (Beijing, China). Phosphate buffered saline (PBS, 0.1 mol/L containing 0.1 mol/L NaCl, pH 7.4) was used as an electrolyte for all electrochemical measurement. Doubly distilled water was used throughout the experiments.

2.2. Apparatus

All electrochemical measurements were performed on a CHI 760D electrochemical workstation (Shanghai CH Instruments Co., China). Transmission electron microscope (TEM) images were obtained from a Hitachi H-800 microscope (Japan). Scanning electron microscope (SEM) images were obtained using field emission SEM (ZEISS, Germany). Electrochemical impedance spectroscopy (EIS) was performed in $[Fe(CN)_6]^{3-/4-}$ working solution in the frequency range of 0.1–10^5 Hz. A conventional three-electrode system was used for all electrochemical measurements: the modified glassy carbon electrode (GCE, 4 mm in diameter) as the working electrode, a saturated calomel electrode (SCE) as the reference electrode, and a platinum wire electrode as the counter electrode.

2.3. Synthesis of Au@mesoporous carbon CMK-3

Au nanoparticles (Au NPs) were prepared according to the reported method (Lu et al., 2002). In brief, it was prepared by the reduction of $AuCl_4^-$ ions using sodium citrate. The typical synthesis procedure is as follows: 100 mL of solution containing 0.01 g $HAuCl_4 \cdot 3H_2O$ was boiled under reflux and 3 mL of a 1% sodium citrate solution was added dropwise while stirring. The boiling solution was then left for another 40 min to cool to room temperature.

About 30 mg mesoporous carbon CMK-3 was added into the above solution and further stirred for 4 h. Finally, the resulting Au@mesoporous carbon CMK-3 was isolated by centrifugation (9000 rpm, 20 min) and dried in vacuum.

2.4. Modification of electrodes

Two primary antibodies were immobilized onto the surface of rGO-TEPA through an amidation reaction between the amine groups attached to rGO-TEPA and the available carboxylic acid of Ab_1. Typically, the solution containing EDC (50 mmol/L) and NHS (50 mmol/L) was added into 1 mL of a solution containing anti-CEA (10 μg/mL) and anti-SCCA (10 μg/mL). The mixture was stirred for 4 h. Then 2 mg rGO-TEPA was added to the above solution. After another 4 h of reaction with stirring, the mixture was centrifuged. The resulting rGO-TEPA-Ab_1 conjugates were re-dispersed in PBS and stored at 4 °C before use.

Fig. 1A showed the procedure to prepare the Au@CMK-3-Ab_2-redox probe conjugate. The as-prepared Au@CMK-3 was dispersed in 1 mL of pH = 7.4 PBS. The solution containing EDC (50 mmol/L) and NHS (50 mmol/L) of anti-CEA was added to the above solution and stirred for 12 h. Then, neutral red solution (2 mg/mL) was added into the mixture. EDC and NHS were used to conjugate Ab_2 with different redox probe (Ab_2-redox probe) by the formation of an amide link between the amino of neutral red and the carboxyl of anti-CEA (Au@CMK-3-anti-CEA-neutral red). The mixture was stirred for 12 h at 4 °C. After centrifugation and washing with PBS, the Au@CMK-3-anti-CEA-neutral red bioconjugates were re-dispersed in PBS and stored at 4 °C before use. The preparation procedure of Au@CMK-3-anti-SCCA-thionine was similar to that of Au@CMK-3-anti-CEA-neutral red.

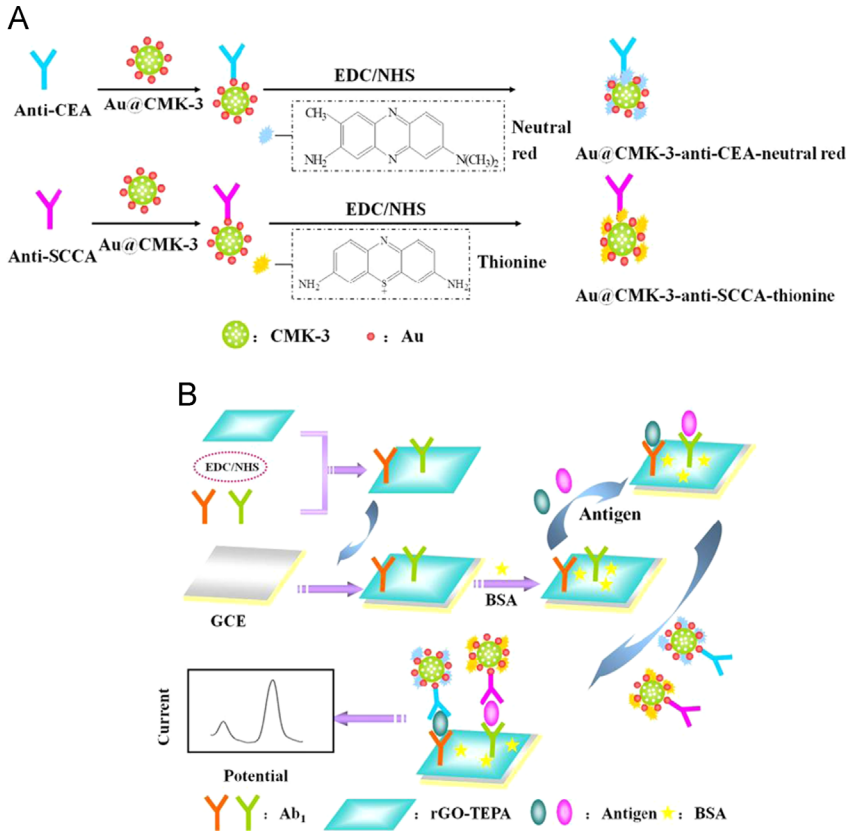

Fig. 1. Fabrication steps of the immunosensor.

The fabrication procedure of the immunosensor is shown in Fig. 1B. GCE was sequentially polished with 1, 0.3, and 0.05 μm alumina powder and then washed ultrasonically in water for a few minutes. After that, 6 μL rGO-TEPA-Ab_1 solutions were added and dried. Next the rGO-TEPA-Ab_1 modified electrode was washed and incubated in 1 wt% BSA solution for 1 h to eliminate nonspecific binding sites. Subsequently a solution containing different concentrations of CEA and SCCA was added onto the electrode surface and incubated for 1 h at room temperature, and then the electrode was washed extensively to remove unbound molecules. Finally, the Au@CMK-3-Ab_2-redox probe buffer solution was dropped onto the electrode surface and incubated for another 1 h. After washing, the electrode was ready for measurement.

3. Results and discussion

3.1. Characterization of rGO-TEPA and Au@mesoporous carbon CMK-3

As shown in Fig. 2A and B, rGO-TEPA with a wrinkled paper-like structure was observed. It had the large surface area in favor of electron transportation. Meanwhile, rGO-TEPA, containing more amino groups, assisted its reaction with Ab_1 through an amidation reaction, thereby increasing the stability of the modified electrodes.

It was confirmed from Fig. 2C that the shape of mesoporous carbon CMK-3 was short rod-like and the pore size distribution was centered at about 5 nm. A large amount of Au nanoparticles were immobilized onto CMK-3 evenly, as shown in Fig. 2D.

3.2. Characterization of the immunosensor

The cyclic voltammetry (CV) characterization of different modified electrodes in 5.0 mmol/L $[Fe(CN)_6]^{3-/4-}$ solution is shown in Fig. S2(A). A pair of typical reversible redox peaks of ferricyanide ions can be observed on the bare GCE (curve *a*). Obviously increased peak current was found on the rGO-TEPA modified GCE (curve *b*), which makes electron transfer easier. When the modified electrode was incubated with Ab_1, peak current obviously decreased for the hinder effect of protein on electron transfer (curve *c*), and the peak current continued to decrease after incubation of BSA (curve *d*) and antigens (curve *e*). However, the peak current increased after incubation of Au@CMK-3-Ab_2-redox probe conjugates (curve *f*), indicating the excellent performance in accelerating electron transfer. Fig. S2(B) exhibits the CV curves of the immunosensor in pH 7.4 PBS. No obvious peak was observed after capture of antigens (curve *a*). However, after the electrode was incubated with Au@CMK-3-Ab_2-redox probe conjugates, two couples of distinct redox peaks were observed (curve *b*), which means Au@CMK-3-Ab_2-redox probe conjugates were immobilized and offered separated redox peaks for detection. Based on above results, we can confirm that the electrode was well-modified.

The stepwise construction process of the immunosensor was also characterized by electrochemical impedance spectroscopy (EIS). EIS is an effective method for probing the features of a modified electrode surface. The impedance spectra consist of a semicircle portion and a linear portion. The semicircle portion corresponds to the electron-transfer-limited process, and the linear portion represents the diffusion-limited process. The semicircle diameter equals the charge transfer resistance R_{ct} (Zhang et al., 2010; Huang et al., 2010a). Fig. 3 illustrates the EIS of different electrodes in the presence of 2.5 mmol/L $[Fe(CN)_6]^{3-/4-}$ containing 0.1 mol/L KCl. Bare GCE had a small semicircle (curve *a*), which is characteristic of a diffusion-limited step in the electrochemical process. When rGO-TEPA was modified onto the electrode, the resistance decreased (curve *b*) a little compared with bare GCE. The reason was that rGO-TEPA has a large effective surface area which promotes electron transfer. After incubation

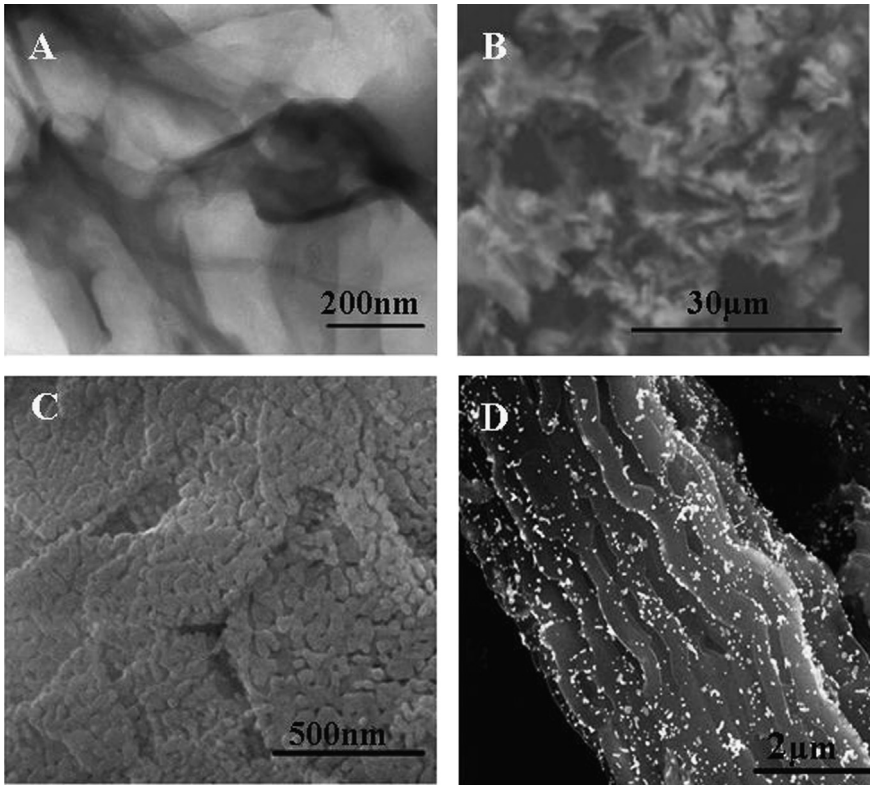

Fig. 2. TEM image of rGO-TEPA (A) and SEM image of rGO-TEPA (B), mesoporous carbon CMK-3 (C), Au@mesoporous carbon CMK-3 (D).

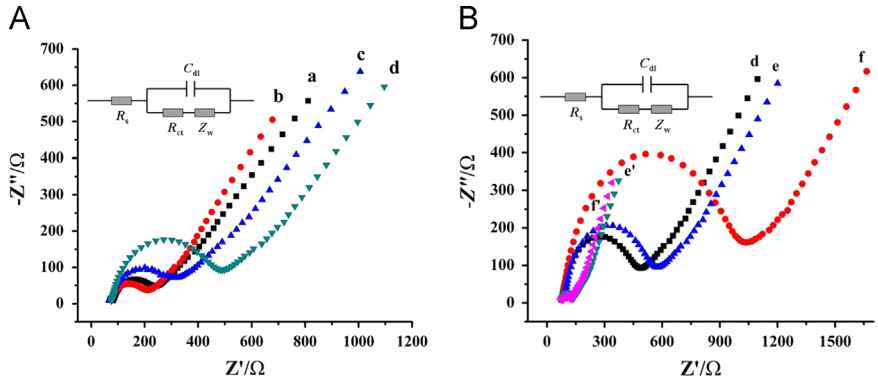

Fig. 3. EIS for each immobilized step in 2.5 mmol/L $[Fe(CN)_6]^{3-/4-}$-0.1 mol/L KCl solution. GCE (a), rGO-TEPA/GCE (b), Ab_1/rGO-TEPA/GCE (c), BSA/Ab_1/rGO-TEPA/GCE (d), curves *e* and *f* were the EIS after the BSA/Ab_1/rGO-TEPA modified electrodes were incubated in the mixture solution containing 15 ng/mL CEA and 15 ng/mL SCCA (e), 20 ng/mL CEA and 20 ng/mL SCCA (*f*), respectively. Curves *e′* and *f′* were the EIS after the sandwich immunoreaction of the corresponding immunosensors.

with Ab_1, the semicircle increased remarkably (curve *c*) because Ab_1 was immobilized on the electrode successfully and blocked the electron transfer. Then a larger semicircle diameter in curve *d* is seen, confirming the high resistance of the electrode interface as the prepared immunosensor is blocked with BSA. Subsequently, R_{ct} increased again (curves *e* and *f*), which indicates the successful capture of antigen and the formation of an immunocomplex layer blocking electron transfer. The higher the concentration of antigen, the greater the resistance value is. When the Au@CMK-3-Ab_2-redox probe (Au@CMK-3-anti-CEA-neutral red and Au@CMK-3-anti-SCCA-thionine) solution was immobilized, R_{ct} decreased greatly (curves *e′* and *f′*). This reason was that the electron mediator and Au were excellent electrically conducting materials, which made electron transfer easier.

The inset of Fig. 3 shows a Randles equivalent circuit which can be used as a model for EIS. The equivalent circuit contains the resistance of solution (R_s), the charge transfer resistance (R_{ct}), the Warburg impedance (Z_W), and the double layer capacitance (C_{dl}), as shown in Table S1. Ideally, Z_W and R_s represent the properties of the electrolyte solution and diffusion of the redox probe, thus they are not affected by modifications occurring on the electrode surface (Huang et al., 2007; Yang and Li, 2005). Throughout the whole processes of electrode modification, the changes in R_{ct} were the most significant among other impedance components. Thus, R_{ct} is a suitable signal for sensing the interfacial properties of the modified glassy carbon electrode.

3.3. Cross-reactivity

An excellent immunosensor for simultaneous multianalyte detection must exclude cross-reactivity between analytes. Therefore, the sensors were used to detect CEA, SCCA and a mixture of

the two analytes, respectively. The response signals were measured by differential pulse voltammetry (DPV) and the results are shown in Fig. 4. Only a peak at −0.62 V (neutral red) is observed when CEA is individually determined (Curve *A*). And when SCCA is individually determined, a peak appears at −0.17 V (thionine) (Curve *B*). When CEA and SCCA are determined simultaneously, there are two peaks at −0.62 V and −0.17 V, respectively (curve *C*). Curves *A* and *B* present favorable consistency with curve *C* in DPV response peak position, signal intensity and appearance, which suggests that the detection of multianalytes would not cause interference with each other and that cross-reactivity between the two analytes was negligible. Therefore, the immunosensor could effectively quantitative detection of each analyte.

3.4. Optimization of experimental conditions

To achieve an optimal electrochemical signaling, the pH value of the substrate solution is an important factor in the electrical current response. The acidity of the solution greatly affects both the activity of the immobilized protein and the electrochemical behavior of the electron mediator. As shown in Fig. 5, it was found that for SCCA, the current response increased from pH 5.5 to 7.4, and it reached the maximum at pH 7.4. Then it decreased from pH 7.4 to 8.1. For CEA, the peak current also reached a maximum at pH 7.4. To maintain a physiological environment and obtain high sensitivity, pH 7.4 PBS was selected for further experiments. The reason was that the highly acidic or alkaline solutions would damage the immobilized protein (Yuan et al., 2004).

Under the optimal condition, a series of immunosensors were prepared for the detection of different concentrations of CEA and SCCA. As shown in Fig. S3, with the increase in concentration, the

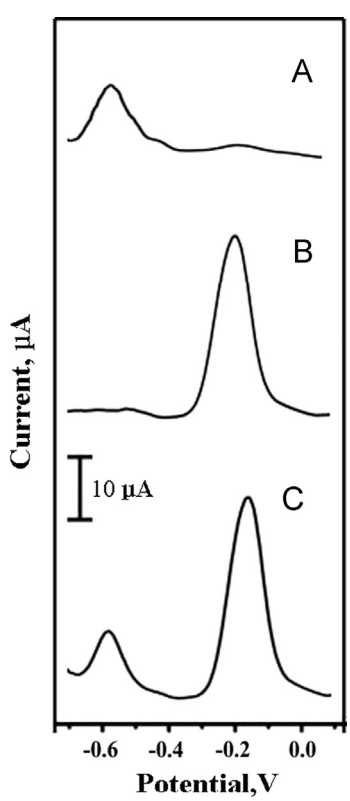

Fig. 4. Differential pulse voltammograms for the investigation of cross-reactivity; (A) 10 ng/mL CEA solution, (B) 10 ng/mL SCCA solution and (C) the mixture solution containing 10 ng/mL CEA and 10 ng/mL SCCA with Au@CMK-3-anti-CEA-neutral red and Au@CMK-3-anti-SCCA-thionine bioconjugates as signal. (For interpretation of the references to color in this figure legend, the reader is referred to the web version of this article.)

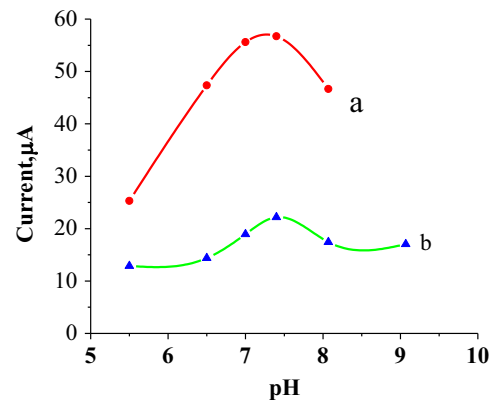

Fig. 5. Effect of pH on the response of the immunosensor to the mixture solution containing 20 ng/mL SCCA (a) and 20 ng/mL CEA (b).

peak currents at −0.62 V (neutral red), and −0.17 V (thionine) increased and were proportional to the concentration of CEA and SCCA, respectively. Hence, the determination of two cervical cancer biomarkers could be carried out based on an increase of the peak currents at −0.62 V and −0.17 V. It can be seen from Fig. 6 that the corresponding linear ranges for CEA and SCCA determination were from 0.05 to 20 ng/mL and 0.03 to 20 ng/mL with detection limits of 0.013 ng/mL and 0.010 ng/mL at $S/N=3$, respectively. The analytical parameters including detection limit and linear range are better or comparable to the results reported for determination of CEA and SCCA, as displayed in Table S2. Therefore, the proposed electrochemical immunosensor showed higher sensitivity.

3.5. Selectivity, reproducibility and stability

Interfering substances such as alpha fetoprotein (AFP), human chorionic gonadotrophin (HCG), human IgG and glucose were added into the detection solution containing 10 ng/mL CEA and 10 ng/mL SCCA. It was found that the immunosensors did not show statistically significant changes (signal change below 5%) of DPV responses after ten times concentration of these potentially co-existing species were added. Thus the selectivity of the immunosensors was acceptable.

To evaluate the fabrication reproducibility of the immunosensors, five electrodes were used for the detection of a mixture containing 10 ng/mL CEA and 10 ng/mL SCCA. The relative standard deviations (RSD) of DPV were 3.3% and 4.8%, respectively, which suggested that the reproducibility of the proposed immunosensors was quite good. When the immunosensor was not in use, it was stored in pH 7.4 PBS at 4 °C. After 5 and 10 days, the current response to the same CEA and SCCA concentration of the immunosensor decreased to about 90% and 84% of its initial value, respectively. Thus, the stability of the immunosensor was also acceptable.

3.6. Serum sample analysis

To further investigate the potential application of the immunosensor for practical analysis, both the amount of CEA and SCCA in the samples and the recovery of the corresponding standard solution were measured. CEA and SCCA contents of serum samples were measured 5 times to obtain the precision. The relative standard deviation (RSD) was calculated and the results were shown in Table S3. After 5.00 ng/mL CEA and 5.00 ng/mL SCCA were added into serum samples, respectively, the average recovery of the immunosensors was calculated and the results were also shown in Table S3. It can be seen from Table S3 that the relative

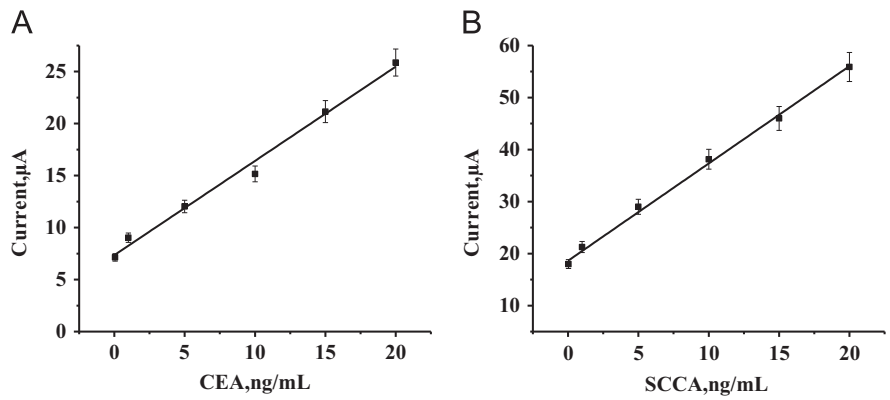

Fig. 6. Calibration curves of CEA (A) and SCCA (B).

standard deviation was in the range of 2.8–3.5% and the recovery was between 96.0–104%. All these presented sufficient precision and high accuracy. Hence, the developed immunoassay methodology could be satisfactorily applied to the determination of CEA and SCCA levels in serum samples.

4. Conclusions

The sensitive detection of two cervical cancer biomarkers was developed using rGO-TEPA as a substrate material and Au@CMK-3-Ab_2-redox probe as labels. The rGO-TEPA was not only used as a substrate for the immobilization of the antibodies, but also promoted the electron transfer of the biosensors. Mesoporous carbon CMK-3 was used to immobilize Au nanoparticles, which was further utilized for the adsorption of the redox probe and secondary antibody. Using CEA and SCCA as model analytes, the sensitive detection was based on the peak current change of neutral red and thionine before and after the antigen–antibody reaction. The proposed immunoassay method showed high sensitivity, negligible cross-reactivity, good selectivity and reproducibility, and acceptable stability, providing potential applications in clinical diagnostics.

Acknowledgements

This study was supported by the Natural Science Foundation of China (No. 21075052, 21175057, 21375047, 21377046), the Natural Science Foundation of Shandong Province (No. ZR2010BQ019), Qin Wei thanks the Special Foundation for Taishan Scholar Professorship of Shandong Province and University of Jinan.

Appendix A. Supplementary material

Supplementary data associated with this article can be found in the online version at http://dx.doi.org/10.1016/j.bios.2013.11.042.

References

Dai, H., Lin, Y., Xu, G., Gong, L., Yang, C., Ma, X., Chen, G., 2012. Electrochim. Acta 78, 508–514.
Gan, T., Hu, C., Chen, Z., Hu, S., 2011. Talanta 85, 310–316.
Geyer, H., Kleine, W., 1987. J. Steroid Biochem 28, 64.
Guo, Z., Hao, T., Du, S., Chen, B., Wang, Z., Li, X., Wang, S., 2013. Biosens. Bioelectron. 44, 101–107.
Hartmann, M., 2005. Chem. Mater. 17, 4577–4593.
Huang, H., Ran, P., Liu, Z., 2007. Bioelectrochemistry 70, 257–262.
Huang, J., Yang, G., Meng, W., Wu, L., Zhu, A., Jiao, X., 2010a. Biosens. Bioelectron. 25, 1204–1211.
Huang, K., Niu, D., Xie, W., Wang, W., 2010b. Anal. Chim. Acta 659, 102–108.
Huang, T., Huang, J., Wei, H., Ho, K., Chu, C., 2013. Biosens. Bioelectron. 43, 173–179.
Kaur, B., Pandiyan, T., Satpati, B., Srivastava, R., 2013. Colloids Surf., B 111, 97–106.
Kjorstad, K.E., Ørjasaeter, H., 1984. Gynecol. Oncol. 19, 284–289.
Kuppan, B., Selvam, P., 2012. Prog. Nat. Sci. 22, 616–623.
Li, H., Cao, Z., Zhang, Y., Lau, C., Lu, J., 2011. Analyst 136, 1399–1405.
Li, X.M., Liu, J.M., Zhang, S.S., 2010. Chem. Commun. 46, 595–597.
Liu, X., Xie, L., Li, H., 2012a. J. Electroanal. Chem. 682, 158–163.
Liu, Y., Dong, X., Chen, P., 2012b. Chem. Soc. Rev. 41, 2283–2307.
Lu, L., Wang, H., Xi, S., Zhang, H., 2002. J. Mater. Chem. 12, 156–158.
Ma, H., Mao, K., Li, H., Wu, D., Zhang, Y., Du, B., Wei, Q., 2013. J. Mater. Chem. B, 5137–5142.
Massuger, L.F.A.G., Koper, N.P., Thomas, C.M.G., Dom, K.E.L., Schijf, C.P.T., 1997. Gynecol. Oncol. 64, 473–476.
Ping, J., Wu, J., Wang, Y., Ying, Y., 2012. Biosens. Bioelectron. 34, 70–76.
Savari, Z., Soltanian, S., Noorbakhsh, A., Salimi, A., Najafi, M., Servati, P., 2013. Sens. Actuators, B 176, 335–343.
Song, Z., Yuan, R., Chai, Y., Zhuo, Y., Jiang, W., Su, H., Che, X., Li, J., 2010. Chem. Commun. 46, 6750–6752.
Sun, B., Zhang, K., Chen, L., Guo, L., Ai, S., 2013. Biosens. Bioelectron. 44, 48–51.
Teymourian, H., Salimi, A., Khezrian, S., 2013. Biosens. Bioelectron. 49, 1–8.
Tian, J., Zhou, L., Zhao, Y., Wang, Y., Peng, Y., Zhao, S., 2012. Talanta 92, 72–77.
Wang, H., Zhang, Y., Li, H., Du, B., Ma, H., Wu, D., Wei, Q., 2013. Biosens. Bioelectron. 49, 14–19.
Wilson, M.S., Nie, W., 2006. Anal. Chem. 78, 6476–6483.
Wu, Y., Zheng, J., Li, Z., Zhao, Y., Zhang, Y., 2009. Biosens. Bioelectron. 24, 1389–1393.
Yang, L., Li, Y., 2005. Biosens. Bioelectron. 20, 1407–1416.
Yuan, R., Tang, D.P., Chai, Y.Q., Zhong, X., Liu, Y., Dai, J.Y., 2004. Langmuir 20, 7240–7245.
Zhang, J.J., Cheng, F.F., Zheng, T.T., Zhu, J.J., 2010. Anal. Chem. 82, 3547–3555.
Zhang, Y., Cheng, Y., Zhou, Y., Li, B., Gu, W., Shi, X., Xian, Y., 2013. Talanta 107, 211–218.
Zhou, M., Ding, J., Guo, L., Shang, Q., 2007a. Anal. Chem. 79, 5328–5335.
Zhou, M., Guo, L., Lin, F., Liu, H., 2007b. Anal. Chim. Acta 587, 124–131.